

Accurate potential energy curves for HeH^+ isotopologues

Cite as: J. Chem. Phys. **137**, 164305 (2012); <https://doi.org/10.1063/1.4759077>

Submitted: 11 June 2012 • Accepted: 01 October 2012 • Published Online: 23 October 2012

Wei-Cheng Tung, Michele Pavanello and Ludwik Adamowicz



View Online



Export Citation

ARTICLES YOU MAY BE INTERESTED IN

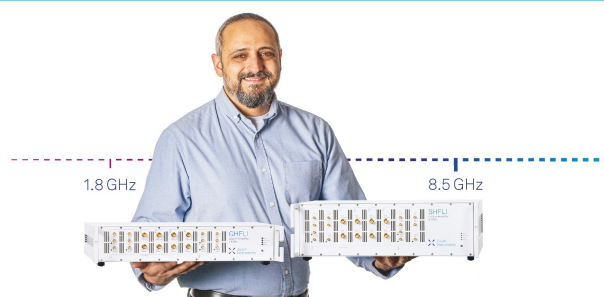
Communication: High precision sub-Doppler infrared spectroscopy of the HeH^+ ion
The Journal of Chemical Physics **141**, 101101 (2014); <https://doi.org/10.1063/1.4895505>

Rovibrational levels of helium hydride ion
The Journal of Chemical Physics **137**, 204314 (2012); <https://doi.org/10.1063/1.4768169>

The $\text{He} + \text{H}_2^+ \rightarrow \text{HeH}^+ + \text{H}$ reaction: Ab initio studies of the potential energy surface, benchmark time-independent quantum dynamics in an extended energy range and comparison with experiments


The Journal of Chemical Physics **137**, 244306 (2012); <https://doi.org/10.1063/1.4772651>





Trailblazers.

Meet the Lock-in Amplifiers that measure microwaves.

 Zurich Instruments

[Find out more](#)

New

Accurate potential energy curves for HeH⁺ isotopologues

Wei-Cheng Tung,¹ Michele Pavanello,² and Ludwik Adamowicz^{1,a)}

¹Department of Chemistry and Biochemistry, University of Arizona, Tucson, Arizona 85721, USA

²Department of Chemistry, Rutgers, The State University of New Jersey, Newark, New Jersey 07102, USA

(Received 11 June 2012; accepted 1 October 2012; published online 23 October 2012)

New accurate ground-state potential energy curves (PEC) for the ⁴HeH⁺, ⁴HeD⁺, ³HeH⁺, and ³HeD⁺ isotopologues are calculated with 600 explicitly correlated Gaussian (ECG) functions with shifted centers in the range between $R = 0.35 a_0$ and $145 a_0$. The calculations include the adiabatic corrections (AC). The absolute accuracy of all Born-Oppenheimer (BO) PEC points is better than 0.0018 cm^{-1} and it is better than 0.0005 cm^{-1} for the ACs. With respect to the very recent BO PEC calculations performed by Pachucki with 20 000 generalized Heitler-London explicitly correlated functions [K. Pachucki, Phys. Rev. A **85**, 042511 (2012)], the present energy calculated at $R = 1.46 a_0$ (a point near the BO equilibrium distance) lies above by only 0.0012 cm^{-1} . Using Pachucki's BO energy at the equilibrium distance of $R = 1.463\,283 a_0$, and the adiabatic corrections calculated in this work for the ⁴HeH⁺, ⁴HeD⁺, ³HeH⁺, and ³HeD⁺ isotopologues, the following values are obtained for their PEC depths: $16\,448.99893 \text{ cm}^{-1}$, $16\,456.86246 \text{ cm}^{-1}$, $16\,451.50635 \text{ cm}^{-1}$, and $16\,459.36988 \text{ cm}^{-1}$, respectively. We also calculate the rovibrational (rovib) frequencies for the four isotopologues using the BO PEC of Pachucki augmented with the present ACs. The improvements over the BO+AC PEC of Bishop and Cheung (BC) [J. Mol. Spectrosc. **75**, 462 (1979)] are 1.522 cm^{-1} at $R = 4.5 a_0$ and 0.322 cm^{-1} at $R = \infty$. To partially account for the nonadiabatic effects in the rovib calculations an effective reduced-mass approach is used. With that, the present ⁴HeH⁺ rovibrational transitions are considerably improved over the BC transitions as compared with the experimental values. Now the rovibrational transitions near the dissociation limit are as well reproduced by the present calculations as the lower transitions. For example, for the ⁴HeD⁺ transitions corresponding to the $\nu = 13$ -9 hot bands the results are off from the experimental values by less than 0.023 cm^{-1} . This confirms high accuracy of the present PECs at larger internuclear separations.

© 2012 American Institute of Physics. [<http://dx.doi.org/10.1063/1.4759077>]

I. INTRODUCTION

HeH⁺ is the simplest heteronuclear ion that comprises the two most abundant elements of the universe. HeH⁺ was first observed by Hogness and Lunn¹ in 1925 and has been extensively studied theoretically and experimentally ever since. From the experimental point of view, the relatively large permanent dipole moment of HeH⁺ allows for measuring its gas-phase rovibrational and pure rotational spectra very precisely. In 1999, Coxon and Hajigeorgiou² used the available experimental rovibrational and pure rotational transitions of ⁴HeH⁺ and its isotopologues, ⁴HeD⁺, ³HeH⁺, and ³HeD⁺, to generate a fitted Born-Oppenheimer (BO) and post-BO potential energy curves (PEC) that agreed with the results of *ab initio* calculations. They used those fitted PECs to determine high-order centrifugal distortion constants, as well as level widths for quasi-bound energy levels. The data employed in the Coxon and Hajigeorgiou analysis were taken from several experimental works. They included the first set of accurate rovibrational transitions of ⁴HeH⁺ ion corresponding to the 1-0 and 2-1 bands measured in 1979 by Tolliver *et al.*³ using an ion-beam laser spectrometer and the accuracy achieved there was 0.002 cm^{-1} . A similar approach was used by Carrington *et al.*^{4,5} to measure the rovibrational transitions of the HeH⁺

isotopologues near the dissociation limits. The measurement of the *P* and *R* branches of the 9-13 hot band of the ⁴HeD⁺ ion⁶ has provided the theorists with a stringent test of the long range behavior of the calculated PEC. The first direct infrared measurement of the absorption spectra of ⁴HeH⁺ by Bernath and Amano⁷ gave nine rovibrational transitions in the 1-0 fundamental band with the accuracy between 0.001 and 0.002 cm^{-1} . Also, the work of Liu *et al.*⁸ and the work of Crofton *et al.*⁹ provided additional rovibrational data for both the fundamental and some hot bands. Besides the rovibrational data, some accurate low and high *J* pure rotational transitions for the $\nu = 0, 1$, and 2 vibrational levels were reported by Matsushima *et al.*¹⁰ and by Liu and Davies.^{11,12} All the data employed by Coxon and Hajigeorgiou² in their analysis are used for testing the calculated transitions obtained in the present work.

On the theoretical side, the first accurate *ab initio* calculation of HeH⁺ ion in the electronic ground state was carried out by Wolniewicz¹³ in 1965. He used a wave function expanded in terms of a 64-term generalized James-Coolidge basis set. However his PEC covered only a relatively narrow range of the molecular bond lengths from $1.1 a_0$ to $1.8 a_0$. Kotos,¹⁴ and Kotos and Peek¹⁵ calculated a long range ($0.9 a_0$ – $9.0 a_0$) BO PEC with a wave function expanded in terms of 83 James-Coolidge basis functions. This PEC was further improved by

^{a)}Electronic mail: ludwik@u.arizona.edu

Bishop and Cheung¹⁶ who used a 255-term wave-function expansion and included adiabatic corrections. Bishop and Cheung employed their improved PEC to calculate the rovibrational energy levels for $v \leq 2$. For three decades the PEC of Cheung and Bishop and their calculated rovibrational transitions have been used for the comparison with the newly measured experimental transitions. Recently, Engel *et al.*¹⁷ used Bishop and Cheung's PEC and the effective reduced masses given by Coxon and Hajigeorgiou,² which partially account for the nonadiabatic effects in the calculation, to recalculate the rovibrational levels. Their results agreed very well with the experimental data.

In 1995, Cencek *et al.*¹⁸ expanded the wave function of HeH^+ ion at the equilibrium molecular bond length in terms of 600 explicitly correlated Gaussian (ECG) functions and lowered the BO energy by 0.9 cm^{-1} with respect to the best previous result. Though they showed that the accuracy of the HeH^+ ion PEC can be further improved, their calculations only concerned a single PEC point. Very recently, Pachucki¹⁹ used 20 000 generalized Heitler-London basis functions to generate a very complete BO PEC with the precision of about $2 \times 10^{-7} \text{ cm}^{-1}$. However, as mentioned by Pachucki,¹⁹ the calculation of the adiabatic corrections with the Heitler-London basis is complicated, and were not performed in his work. These corrections are known to contribute about 7.9 cm^{-1} to the $^4\text{HeH}^+$ PEC.¹⁶ To have the calculated rovibrational transitions converging to the experimental data, the adiabatic corrections are the first among the post-BO corrections that should be included in the PEC. The calculation of these corrections for the full range of the PEC and the use of the BO PEC of Pachucki augmented with the corrections to determine the rovibrational transitions for $^4\text{HeH}^+$ and its isotopologues are the main goals of the present work.

We should also mention the very accurate calculations of pure vibrational states of $^4\text{HeH}^+$ performed in our group without assuming the BO approximation^{20,21} and with including the relativistic corrections.^{22,23} For the two lowest pure vibrational transitions the results were only off from the experimental values by $0.0172\text{--}0.0190 \text{ cm}^{-1}$. The difference was attributed to not including the quantum electrodynamics (QED) corrections in the PEC.

The computational approach developed in our previous works^{24–27} is employed in the present work. The approach does not include the relativistic and QED effects. Thus, even though one can expect these effects to be very small for HeH^+ , their omission constitutes the major source of error in the present rovibrational calculations.

II. THE METHOD

A. The wave function

We use the variational method to calculate the HeH^+ ground-state electronic wave function and the corresponding BO energy. The spatial part of the electronic wave function is a linear combination of basis functions:

$$\Psi(\mathbf{r}) = \sum_{k=1}^M c_k \phi_k(\mathbf{r}), \quad (1)$$

where M is the size of the basis set, c_k are the linear expansion coefficients, and ϕ_k are the following all-electron ECGs with floating centers, \mathbf{s}_k :

$$\phi_k(\mathbf{r}) = \exp[-(\mathbf{r} - \mathbf{s}_k)'(\mathbf{A}_k \otimes \mathbf{I}_3)(\mathbf{r} - \mathbf{s}_k)]. \quad (2)$$

In the ground-state calculation of HeH^+ the Gaussian centers are only allowed to float along the bond axis. Floating the centers adds flexibility to the Gaussians in describing the molecular electronic state. In Eq. (2), \mathbf{r} is the $3n$ -dimensional vector of the electron Cartesian coordinates and \mathbf{s}_k is a $3n$ -dimensional shift vector of the Gaussian centers, with n being the number of electrons. \mathbf{A}_k is a $n \times n$ symmetric matrix. To carry out matrix-vector multiplications related to the derivation of the Hamiltonian and overlap matrix elements, \mathbf{A}_k is expanded to the dimension of $3n \times 3n$ using the Kronecker product, \otimes , of \mathbf{A}_k with the 3×3 identity matrix, \mathbf{I}_3 . For $\phi_k(\mathbf{r})$ to be square integrable, \mathbf{A}_k has to be a positive definite matrix. This automatically happens if \mathbf{A}_k is represented in the Cholesky-factorized form as: $\mathbf{A}_k = \mathbf{L}_k \mathbf{L}_k'$, where \mathbf{L}_k is a lower triangular matrix and \mathbf{L}_k' is its transpose.²⁸ As the elements of \mathbf{L}_k can vary from $-\infty$ to $+\infty$, they are convenient variables to be used in the variational energy minimization because their optimization can be carried out without any constraints.

The total electronic wave function has to be antisymmetric with respect to all permutations of the electron labels, P_{ij} , where P_{ij} permutes the labels of the i th and j th electrons. To satisfy this requirement, a permutation operator $\hat{P} = \hat{Y}^\dagger \hat{Y}$ (the dagger stands for conjugate) is applied to each ECG, where \hat{Y} is the Young projection operator which is a linear combination of permutation operators, \hat{P}_γ . The Young operator can be derived using the appropriate Young tableaux representing the electronic $^1\Sigma$ ground state of HeH^+ ion. For this state the Young operator is: $\hat{Y} = (\hat{1} + \hat{P}_{12})$, where $\hat{1}$ is the identity operator. The \hat{P}_{ij} operator can be represented as a $n \times n$ permutation matrix applied to \mathbf{A}_k matrix and a $3n \times 3n$ permutation matrix applied to \mathbf{s}_k vector. As the Hamiltonian is invariant with respect to all permutations of the electronic labels, in the calculation of the Hamiltonian and overlap matrix elements \hat{P} is applied to the *ket* only.

The variational optimization of the wave function is carried out by minimizing the Rayleigh quotient:

$$E = \frac{\langle \Psi | \hat{H} | \Psi \rangle}{\langle \Psi | \Psi \rangle}. \quad (3)$$

It involves optimizing the linear (c_k) coefficients in Eq. (1) and the nonlinear \mathbf{L}_k and \mathbf{s}_k parameters in Eq. (2). The nonlinear parameters are optimized using a quasi-Newton procedure and the optimal linear parameters are obtained by solving the secular equation in each optimization step. To accelerate the optimization process, the analytical energy gradient determined with respect to the \mathbf{L}_k and \mathbf{s}_k parameters is evaluated in our calculations and provided to the quasi-Newton optimization procedure. The availability of the gradient considerably accelerates the optimization process. The norm of the gradient is also calculated to determine how well converged is the energy. If this norm is smaller than 10^{-12} a.u. the optimization is terminated.

The initial wave function is calculated with 600 ECG basis functions at the HeH^+ equilibrium bond length. By

incrementally extending and contracting the internuclear distance and reoptimizing the basis set at each PEC point a complete BO PEC is generated.

B. Calculating the adiabatic correction

The BO approximation fixes the nuclear positions and ignores the coupling between the electronic and nuclear motions. This deficiency can be remedied by including in the PEC the adiabatic and nonadiabatic corrections. A procedure to determine the adiabatic correction was proposed by Cencek and Kutzelnigg.²⁹ In the procedure the adiabatic correction is expressed as the expectation value of the nuclear kinetic energy operator with the electronic BO wave function. However, the ECG BO wave function only explicitly depends on the electronic coordinates, but not on the nuclear coordinates (even parametrically). This precludes its direct differentiation with respect to the nuclear coordinates in calculating the expectation value. A way around it is to use the following approximate numerical differentiation approach:

$$\frac{\partial \Psi}{\partial Q_{i\alpha}} \simeq \frac{\Psi(Q_{i\alpha} + \frac{1}{2}\Delta Q_{i\alpha}) - \Psi(Q_{i\alpha} - \frac{1}{2}\Delta Q_{i\alpha})}{\Delta Q_{i\alpha}}, \quad (4)$$

where $Q_{i\alpha}$ is the i th nuclear coordinate of the α nucleus and $\Delta Q_{i\alpha}$ is its finite displacement. In Eq. (4), instead of directly calculating $\Psi(Q_{i\alpha} - \frac{1}{2}\Delta Q_{i\alpha})$ and $\Psi(Q_{i\alpha} + \frac{1}{2}\Delta Q_{i\alpha})$, the Gaussian product theorem²⁹ is used to adjust the centers of the ECGs, s_k , to the $\pm \frac{1}{2}\Delta Q_{i\alpha}$ displacement of the Q_i coordinate of the i th nucleus. The method involves decomposing a Gaussian not centered on a nucleus into a product of two Gaussians centered on different nuclei, then moving these two Gaussians with the nuclei, as they are shifted, and reassembling the original single Gaussian from the two moved nuclei-centered Gaussians. After the centers are adjusted, the secular equation is solved to determine the wave function, *i.e.* new linear expansion parameters (c_k) are determined. Using the above approximate numerical derivative of the wave function in the following Born-Handy formula³⁰ one obtains the adiabatic correction as

$$\begin{aligned} E_{\text{ad}} &= \langle \Psi | -\frac{1}{2} \sum_{\alpha=1}^K \frac{1}{M_{\alpha}} \sum_{i_{\alpha}=1}^3 \frac{\partial^2}{\partial Q_{i\alpha}^2} | \Psi \rangle \\ &= \frac{1}{2} \sum_{\alpha=1}^K \sum_{i_{\alpha}=1}^3 \frac{1}{M_{\alpha}} \left\langle \frac{\partial \Psi}{\partial Q_{i\alpha}} \left| \frac{\partial \Psi}{\partial Q_{i\alpha}} \right. \right\rangle \\ &= \sum_{\alpha=1}^K \sum_{i_{\alpha}=1}^3 \frac{1}{M_{\alpha}} \frac{1-S}{\Delta Q_{i\alpha}^2}, \end{aligned} \quad (5)$$

$$S = \left\langle \Psi \left(Q_{i\alpha} - \frac{1}{2}\Delta Q_{i\alpha} \right) \left| \Psi \left(Q_{i\alpha} + \frac{1}{2}\Delta Q_{i\alpha} \right) \right. \right\rangle, \quad (6)$$

where M_{α} is the mass of nucleus α (7294.299 536 $3m_e$ for the ^4He nucleus, 5495.885 269 m_e for the ^3He nucleus, 1836.152 672 $61m_e$ for the H nucleus, and 3670.482 965 $4m_e$ for the D nucleus,³¹ where $m_e = 1$ is the electron mass) and K is the number of nuclei in the system. The numerical differentiation and the Gaussian product theorem work best when $\Delta Q_{i\alpha}$ is

small. The smaller the $\Delta Q_{i\alpha}$ ($< 10^{-5} a_0$) value the more accurate the adiabatic correction determined using Eq. (5) should be. However, as evident in Eqs. (5) and (6), when the value of $\Delta Q_{i\alpha}$ is very small, the wave functions in *bra* and *ket* become very similar and the value of the overlap (S) approaches one. When this happens, one loses the numerical precision in the calculation of the term $\frac{(1-S)}{\Delta Q_{i\alpha}^2}$. Thus, a balanced value of $\Delta Q_{i\alpha}$ needs to be used.

Let us now examine the accuracy of the adiabatic correction calculated using the above-described approach for HeH^+ . As the HeH^+ ion dissociates to a He atom and a proton, all electrons localize at the He nucleus and none is found around the bare proton. As the adiabatic correction for a bare proton is zero, one can check if near zero values are indeed obtained for the proton contribution to the HeH^+ adiabatic correction at large internuclear distances. The results show that in the present calculations the proton contribution to the HeH^+ adiabatic correction converges to zero as $R \rightarrow \infty$.

Tests performed for different values of $\Delta Q_{i\alpha}$ showed that its optimal value should be around $5 \times 10^{-6} a_0$. However, even for this value, the adiabatic correction of the proton at large internuclear separations shows some random oscillations with the magnitude of about $2 \times 10^{-3} \text{ cm}^{-1}$ limiting the overall accuracy of the correction to about $2 \times 10^{-2} \text{ cm}^{-1}$. There are two ways to remedy this accuracy drop. First, instead of using Eq. (4), one can use a five-point (or more-point) stencil to improve the precision in the numerical differentiation. The second option is to increase the precision of calculating the adiabatic correction from the double precision (64 bit) used in our previous works^{25,26} to the quadruple precision (128 bit). Both options are tested in the present work. For the first option, we find the improvement of the precision due employing the five-point stencil to be rather limited and insufficient. Therefore, we employ the second option which turns out to be much better. As Table II shows, the proton contribution to the adiabatic correction calculated with the quadruple precision for HeH^+ at the $R = 145 a_0$ internuclear distance is now reduced to only $2.92734 \times 10^{-11} \text{ cm}^{-1}$ when calculated with $\Delta Q_{i\alpha} = 1 \times 10^{-8} a_0$. This is much closer to zero than calculated with the double precision. Thus, by recalculating the adiabatic corrections for all PEC points with the quadruple precision their absolute accuracy is now close to that of the BO energies. The BO PEC energies and the corresponding ACs calculated in the $R = 0.9 a_0$ – $145 a_0$ range of the internuclear distance are given in the supplementary materials.³²

C. Account for the nonadiabatic effect in the calculation of the rovibrational level

The adiabatic correction provides only the leading correction accounting for the coupling of the motions of the electrons and the nuclei. It does not account for the fact that, when the molecule vibrates or/and rotates, not only the nuclei but also the electrons (or a part of the electrons) participate in these motions³³ by moving with the nuclei. To account for this effect one needs to include nonadiabatic corrections in the calculation. An effective approach was proposed by Bunker and Moss.^{34,35} It uses the

following effective vibration-rotation Hamiltonian:

$$\left\{ -\frac{\hbar^2}{2\mu_{\text{vib}}} \frac{d^2}{dR^2} + \left[V(R) + \frac{\hbar^2 J(J+1)}{2\mu_{\text{rot}} R^2} \right] \right\} \Psi_{v,J}(R) = E_{v,J} \Psi_{v,J}(R), \quad (7)$$

where $V(R)$ is the molecular PEC, R is the internuclear distance, and $E_{v,J}$ and $\Psi_{v,J}(R)$ are the vibration-rotation energy and the rovibrational wave function, respectively. $\Psi_{v,J}(R)$ depends on the vibration and rotation quantum numbers, v and J , μ_{vib} is the effective vibrational reduced mass, and μ_{rot} is the effective rotational reduced mass. These effective reduced masses, which in general are not equal to each other, approximately account for the nonadiabatic effects in the vibrational and rotational kinetic-energy operators in the Hamiltonian. Though the effective reduced masses should, in principle, depend on the internuclear distance,^{33,34} in the first approximation one can neglect this dependency and use for them constant values. This is what has been done in the present calculations. The LEVEL 8.0 program of Le Roy³⁶ is used here to solve the vibration-rotation Eq. (7) numerically and to determine the rovibrational energy levels.

III. RESULTS AND DISCUSSION

To converge the calculated rovibrational transition frequencies to the corresponding experimental values one needs an accurate PEC that includes very accurately calculated BO energies, as well as the adiabatic, nonadiabatic, relativistic, and QED corrections. In the present work, we adopt the BO PEC of Pachucki¹⁹ and add to it the adiabatic corrections calculated in this work for all HeH⁺ isotopologues. We partially account for the nonadiabatic effects by using effective reduced masses. The relativistic and QED corrections are excluded, which is the largest source of error in the present calculations. We discuss the results obtained in the calculations in Secs. III A–III C.

A. Evaluating the accuracy of the PEC

Even though we use Pachucki's BO PEC to calculate rovibrational transitions, we find it interesting to examine how accurately the PEC is represented in the present ECG calculations. First we compare the present BO energies obtained at the equilibrium molecular bond length with the energies of

TABLE I. Convergence of the BO energy at the equilibrium internuclear distance of $R = 1.46 a_0$ in the present work and in the best previous ECG calculations of Cencek *et al.*¹⁸ Energies are in E_h .

Basis size (M)	This work	Cencek <i>et al.</i> ¹⁸
75	−2.978 690 883	−2.978 687 434
150	−2.978 705 727	−2.978 705 281
300	−2.978 706 577	−2.978 706 516
600	−2.978 706 595	−2.978 706 591
1200	−2.978 706 598	...
Exact value	−2.978 706 600 ^a	

^aThis value is calculated using over 20 000 Heitler-London basis functions by Pachucki.¹⁹

Cencek *et al.*¹⁸ As shown in Table I, our BO energies converge faster than theirs for $M \leq 300$. We attribute this to the use of the analytical gradient in optimizing the ECG nonlinear parameters in this work.^{25,26} Improved computational capabilities are also contributing to the increase of the optimization efficiency. With 600 ECGs both calculations converge to similar values with our energy being slightly lower by about $4 \times 10^{-9} E_h$ than Cencek's *et al.* With 600 ECGs the basis set is almost saturated and this explains why the two calculations converge to similar energies. To confirm that this is indeed the case we incrementally add more functions to the basis set until the basis size reaches 1200 ECGs. The additional 600 functions lower the BO energy by only $3 \times 10^{-9} E_h$. This energy is only off from the most accurate value calculated with 20 000 Heitler-London basis functions by Pachucki by $2 \times 10^{-9} E_h$.¹⁹ Though the accuracy can be further improved in our calculations by adding more Gaussians to the basis set, the error due to not accounting for the relativistic and QED effects is significantly larger than the error in the BO energies. A similar conclusion stopped the addition of more ECGs to the basis set in our previous works.^{25,26} Hence, the $M = 600$ basis set is chosen to carry out the HeH⁺ PEC calculations.

Two PEC points, $R = 1.46 a_0$ and $R = 145 a_0$, and the corresponding adiabatic corrections, both shown in Table II, are used to evaluate the accuracy of the present PEC. At dissociation HeH⁺ becomes an isolated He atom and a bare proton and its BO energy is equal to the energy of a He atom. This energy can be taken, for example, from the BO calculations of Stanke *et al.*³⁷ where the He wave function was expanded in terms of 1500 ECGs and where the accuracy of the

TABLE II. Accuracy evaluation of the HeH⁺ BO energies and the corresponding adiabatic correction at $R = 145 a_0$ and $R = 1.46 a_0$. The present BO energies (in units of E_h) are shown with an extra digit.

	Estimation of exact value	This work	$\Delta(\text{cm}^{-1})$
$E_{\text{BO}}(\text{He})$	−2.903 724 377 0 ^a		
$E_{\text{BO}}(\text{H}^+)$	0.000 000 000 0		
$E_{\text{BO}}(\text{He-H}^+)(R = \infty)$	−2.903 724 377 0	−2.903 724 377 4 ^b	−0.00008
$E_{\text{ad}}(^4\text{He})$	0.000 419 888 7 ^c	0.000 419 888 7	-2.77734×10^{-8}
$E_{\text{ad}}(\text{H}^+)$	0.000 000 000 0	1.33379×10^{-16}	2.92734×10^{-11}
$E_{\text{BO}}(\text{He-H}^+)(R = 1.46 a_0)$	−2.978 706 600 3 ^d	−2.978 706 594 9	0.00119

^aThis value is given in Ref. 37.

^bObtained at $R = 145 a_0$.

^cThis value is estimated by $E_{\text{ad}}(^4\text{He}) = \frac{\langle p_1, p_2 \rangle - E_{\text{BO}}(\text{He})}{M_{\alpha}(^4\text{He})}$, where $\langle p_1 \cdot p_2 \rangle = 0.159\,069\,475\,085\,84 \text{ a.u.}$ ³⁸

^dThis value is the BO energy calculated with 20 000 Heitler-London basis functions by Pachucki.¹⁹

TABLE III. Convergence of the adiabatic correction of ${}^4\text{HeH}^+$ with respect to the basis set size at selected internuclear distances. The correction is in cm^{-1} .

Basis size (M)	Internuclear distance (a_0)									
	0.9		1.2		1.46		3.0		145	
	${}^4\text{He}$	H	${}^4\text{He}$	H	${}^4\text{He}$	H	${}^4\text{He}$	H	${}^4\text{He}$	H
75	84.75945	34.15264	83.89289	22.11908	84.33984	15.74190	90.55128	1.99005	92.15490	3.91151×10^{-11}
150	84.90728	34.75978	84.02855	22.51361	84.46644	15.79622	90.59988	1.99601	92.15491	3.41961×10^{-11}
300	84.92583	34.77104	84.04964	22.52322	84.47944	15.80334	90.60817	1.99641	92.15491	3.39655×10^{-11}
600	84.92740	34.77183	84.05181	22.52401	84.48256	15.80394	90.61216	1.99661	92.15491	2.92734×10^{-11}
1200	84.92750	34.77194	84.05217	22.52412	84.48298	15.80397	90.61228	1.99662	92.15491	2.97958×10^{-11}

corresponding He energy was estimated to be around 10^{-12} E_h . The difference of the BO energies between the He atom and the HeH^+ ion at $R = 145 a_0$ obtained in the present work is only $-8 \times 10^{-5} \text{ cm}^{-1}$. We should emphasize that this small negative difference is not a result of inaccuracies of the calculations, but it is due to the weak interaction between the He atom and the proton which is still not zero even at this large internuclear separation. The results of Pachucki¹⁹ also show this interaction, which in his calculations at the internuclear distance of $R = 60 a_0$ is equal to $-1.17181 \times 10^{-2} \text{ cm}^{-1}$.

The accuracy of the adiabatic correction at $R = 145 a_0$ is evaluated in a similar way by summing the adiabatic correction of the He atom and that of the proton (which is zero). As shown in Table II, the HeH^+ absolute accuracy of the adiabatic correction due to the proton and the ${}^4\text{He}$ at $R = 145 a_0$ are 2.92734×10^{-11} and $-2.77734 \times 10^{-8} \text{ cm}^{-1}$, respectively. To estimate the accuracy of the adiabatic corrections at shorter distances than $R = 145 a_0$, the convergence of the corrections with respect to the basis set size is examined for several selected PEC points. The analysis is shown in Table III. As one can see in Table III, the value of the correction calculated with $M = 600$ basis at and around the equilibrium internuclear distance is off from the value calculated with $M = 1200$ basis by only about $4 \times 10^{-4} \text{ cm}^{-1}$.

To evaluate the absolute accuracy of the BO energy at the equilibrium molecular bond length, our value calculated with 600 ECGs is compared with the value of Pachucki¹⁹ calculated with over 20 000 Heitler-London basis functions. The difference of these two values of 0.00118 cm^{-1} provides an estimate of the absolute accuracy obtained at the equilibrium molecular bond length in the present calculations.

As mentioned, at the internuclear distance of $R = 145 a_0$, the BO energy of HeH^+ is still below the BO energy of the He atom. Thus this point cannot be used to evaluate the accuracy of the PEC at larger internuclear distances. One can expect that a same-size ECG basis set should give slightly better absolute accuracy of the molecular energy near dissociation than at the equilibrium, because it is easier to describe almost isolated atoms (a helium atom in the case of dissociated HeH^+) than a strongly bonded system (HeH^+ at equilibrium). Therefore, the absolute accuracy of the PEC point at $R = 145 a_0$ is likely higher than at the equilibrium bond length, where it is equal to 0.00118 cm^{-1} and the same trend is also expected to be observed for the adiabatic correction. To confirm this, we compare our and Pachucki's BO PECs in Figure 1.

The figure shows that indeed the difference of the two PECs is larger for short internuclear distances than for longer ones. Beyond $R = 9 a_0$ the two PECs become nearly parallel with the difference between them of about 0.00026 cm^{-1} (the value of the difference at $R = 60 a_0$). Thus the relative accuracy difference between the equilibrium bond length and the dissociation limit can be estimated as 0.00093 cm^{-1} , with, as mentioned, the latter being more accurate. Our BO PEC shows some oscillations of the magnitude of about $5 \times 10^{-5} \text{ cm}^{-1}$ particularly at shorter internuclear distances. We attribute these oscillations to linear dependencies which occasionally occur in the calculations. Our dealing with this issue involves identifying the linearly dependent functions usually appearing in pairs and replacing one of the function in each pair with a new function optimized to have maximum overlap with the pair.^{24,25} Usually after the replacement and subsequent reoptimization of the whole basis set the energy goes back to a similar value as it was before the replacement. With this treatment the oscillations subside. However, small energy oscillations are unavoidable, especially for shorter internuclear distances, because the wave function of the molecule is harder to describe in this region using a limited fixed number of basis functions. The size of the basis set which is quite adequate for longer distances may be slightly less complete for shorter distances leading to some small energy oscillations. The energy oscillations usually become smaller when the basis set becomes more complete. While the oscillation problem can be corrected by using a larger

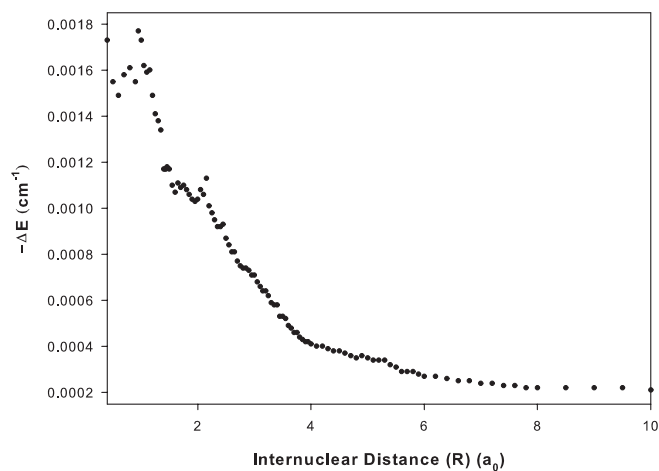
FIG. 1. Comparison of the present and Pachucki's¹⁹ BO PECs.

TABLE IV. Contribution of the adiabatic correction (ΔE_{ad}) to the PEC depth (D_e) for different HeH^+ isotopologues. The BO PEC depth of Pachucki¹⁹ is 16 457.07122 cm^{-1} . All quantities are in cm^{-1} .

	ΔE_{ad}	D_e
$^4\text{HeH}^+$	− 8.07229	16 448.99893
$^4\text{HeD}^+$	− 0.20876	16 456.86246
$^3\text{HeH}^+$	− 5.56487	16 451.50635
$^3\text{HeD}^+$	2.29866	16 459.36988

basis set, their magnitude in the HeH^+ PEC obtained with 600 ECGs are much smaller than the PEC accuracy and thus they do not constitute a problem.

The PECs of the following four HeH^+ isotopologues: $^4\text{HeH}^+$, $^4\text{HeD}^+$, $^3\text{HeH}^+$, and $^3\text{HeD}^+$ have been generated by adding the corresponding adiabatic corrections to the most accurate to date BO HeH^+ PEC of Pachucki.¹⁹ We also added the adiabatic corrections to his HeH^+ BO energy obtained at the equilibrium internuclear distance of $R = 1.463\,283\,a_0$ to determine the potential energy depths (D_e) for the isotopologues. The results are shown in Table IV. As can be seen in the table, the potential depths for $^4\text{HeH}^+$, $^4\text{HeD}^+$, and $^3\text{HeH}^+$ decrease relative to the BO value, but the depth for $^3\text{HeD}^+$ increases. This variability results from the interplay between the He and H isotopic contributions to the adiabatic correction. The increasing isotopic mass of He shallows the potential, while the increasing mass of H deepens it.

B. Accounting for the nonadiabatic effect

In our previous calculations concerning He_2^+ it was reasonable to assume an even distribution of the three electrons among the two nuclei and to determine the effective reduced nuclear masses accordingly. However, for heteronuclear diatomic molecules, such as HeH^+ , where the electron distribution is not symmetric, a different approach needs to be applied. In some works an empirical approach has been used where the effective vibrational and rotational reduced masses, μ_{vib} and μ_{rot} in Eq. (7), are determined by fitting the calculated rovibrational transition energies to the experimental data. However, the experimental data involve two additional types of effects, the relativistic effects and the QED effects, and adjusting the reduced masses, which only suppose to correct for the nonadiabatic effects, to fit the experimental data is not strictly correct. Also the approach with empirically adjusted reduced masses loses its *ab initio* quality.

In the present approach we determine the effective vibrational reduced nuclear masses for HeH^+ by minimizing the difference between the transition energy of the lowest pure vibrational transition of $^4\text{HeH}^+$ obtained in the present calculations and the previous non-BO calculations.²³ The effective vibrational reduced mass, μ_{vib} , is defined as

$$\mu_{\text{vib}} = \frac{(m_{\text{He}^{+2}} + x \times m_e)(m_{\text{H}^+} + y \times m_e)}{(m_{\text{He}^{+2}} + x \times m_e) + (m_{\text{H}^+} + y \times m_e)} \text{ with } x + y = 2, \quad (8)$$

where $m_{\text{He}^{+2}}$ is the nuclear mass of the He atom, m_{H^+} is the nuclear mass of the H atom, m_e is the electron mass, and x and y are the electron populations at the He and H nuclei,

respectively. The procedure involves guessing some initial values of x and y , determining the effective vibrational reduced mass with them, and using the reduced mass to solve the nuclear Schrödinger equation. Next x and y are adjusted and the nuclear Schrödinger equation is solved again. This continues till the calculated lowest pure vibrational transition best matches the value obtained from the non-BO calculation. The procedure leads to the x and y values being 1.84165 and 0.15835, respectively. These values indicate that, when the HeH^+ molecule vibrates in low vibrational states, 92% of the electron mass moves with the He nucleus and 8% moves with the H nucleus.

For the effective vibrational and rotational reduced masses, μ_{vib} and μ_{rot} , Bunker *et al.*³⁵ give the following expressions: $\mu_{\text{rot}} = \mu/(1 + \alpha)$ and $\mu_{\text{vib}} = \mu/(1 + \beta)$, where the values of α and β are small constants dependent of the system and μ is the reduced mass calculated using the nuclear masses. For example, for H_2 and D_2 α is equal to −0.000 045 and β is equal to −0.000 253. Thus, as the effective rotational reduced mass is much closer to μ than the effective vibrational reduced mass, μ_{rot} can be set equal to μ . This is done in the calculations of the rotational states in the present work.

The pure vibrational transitions calculated in our previous nonadiabatic and the present adiabatic calculations are compared in Table V. As one can see, the difference between the two sets of transitions is smaller than 0.01 cm^{-1} , except the 8-7 transition that shows a difference of 0.0184 cm^{-1} . This indicates that, even though the reduced masses were determined based on the lowest vibrational transition, they are also good for higher transitions. The larger discrepancy for the 8-7 vibrational transition is expected, because the effective reduced masses are assumed to be independent on the internuclear distance and, as they are optimized for the lowest transition, they should be more correct for low-amplitude vibrations than for high-amplitude ones.

The determination of the rovibrational energy levels by solving the vibration-rotation equation (Eq. (7)) using the LEVEL program involves the following four steps. In the

TABLE V. Comparison of nonrelativistic $v' \rightarrow v''$ vibrational frequencies between the adiabatic and nonadiabatic calculations. The following three sets of masses for the ^4He and H nuclei are used in the vibrational level calculations: the nuclear masses (nucl), the effective masses (eff, see text), and the atomic masses (at). All values are in cm^{-1} .

$v' \rightarrow v''$	$E_{\text{non-Ad}}^{23}$	Difference		
		μ_{nucl}	μ_{eff}	μ_{at}
1→0	2911.0174	0.1558	0.0000	0.0840
2→1	2604.2053	0.1242	0.0052	0.0694
3→2	2295.6350	0.0898	0.0083	0.0523
4→3	1982.1338	0.0516	0.0090	0.0320
5→4	1660.4510	0.0053	0.0038	0.0046
6→5	1327.9060	− 0.0414	0.0008	− 0.0220
7→6	984.4969	− 0.0958	− 0.0093	− 0.0560
8→7	639.3449	− 0.1416	− 0.0184	− 0.0849
9→8	327.4952	− 0.1339	− 0.0070	− 0.0754
10→9	116.2242	− 0.0798	− 0.0002	− 0.0431
11→10	24.4392	− 0.0274	0.0026	− 0.0136

TABLE VI. Comparison of the $^4\text{HeH}^+$ experimental pure rotational transitions with the values obtained in the present work and the values calculated by Bishop and Cheung.¹⁶ ΔE is the difference between the calculations. All units are in cm^{-1} .

ν	J''	J'	Experiment frequency	Bishop and Cheung	This work	ΔE	ν	J''	J'	Experiment frequency	Bishop and Cheung	This work	ΔE
0	0	1	67.053 ^a	−0.001	−0.001	0.000	1	13	14	704.270 ^c	−0.018	−0.022	−0.005
	1	2	133.717 ^a	−0.002	−0.002	0.000		14	15	731.430 ^c	−0.015	−0.019	−0.004
	6	7	448.160 ^b	−0.012	−0.006	0.006		15	16	754.235 ^c	−0.018	−0.022	−0.004
	10	11	657.221 ^c	−0.027	−0.016	0.011		16	17	772.464 ^c	−0.017	−0.018	−0.002
	11	12	701.317 ^c	−0.019	−0.009	0.010		17	18	785.837 ^c	−0.014	−0.013	0.001
	12	13	741.706 ^c	−0.026	−0.014	0.012		18	19	793.997 ^c	−0.023	−0.019	0.004
	13	14	778.224 ^c	−0.033	−0.018	0.015		19	20	796.490 ^c	−0.027	−0.019	0.009
	14	15	810.708 ^c	−0.038	−0.023	0.014		20	21	792.616 ^c	−0.030	−0.021	0.009
	15	16	839.010 ^c	−0.042	−0.027	0.015		21	22	781.245 ^d	−0.045	−0.033	0.012
	16	17	862.984 ^c	−0.043	−0.028	0.015		22	23	760.340 ^e		−0.022	
	17	18	882.475 ^c	−0.046	−0.032	0.014		23	24	724.933 ^d		−0.016	
	18	19	897.334 ^c	−0.036	−0.022	0.015	2	13	14	627.320 ^c	−0.018	−0.014	0.004
	20	21	912.242 ^c	−0.035	−0.028	0.007		14	15	648.324 ^c	−0.011	−0.011	0.000
	21	22	911.704 ^c	−0.033	−0.028	0.005		15	16	664.559 ^c	−0.015	−0.014	0.000
	23	24	891.888 ^d	−0.033	−0.035	−0.003		16	17	675.609 ^c	−0.013	−0.013	0.000
	24	25	870.298 ^d		−0.038			17	18	680.895 ^c	−0.012	−0.014	−0.002
	25	26	837.180 ^d		−0.038			18	19	679.586 ^c	−0.017	−0.016	0.001
1	10	11	598.829 ^c	−0.014	−0.016	−0.002		19	20	670.340 ^c	−0.021	−0.012	0.009
	11	12	637.767 ^c	−0.011	−0.014	−0.004		20	21	650.613 ^d		0.007	
	12	13	672.989 ^c	−0.097	−0.103	−0.006							
RMSE ^f											0.031	0.026	

^aMatsushima *et al.*¹⁰^bLiu *et al.*⁸^cLiu and Davies.¹²^dLiu and Davies.¹¹^eHoyland.³⁹^fRoot-mean-square error.

first step, the pure vibrational levels are calculated with the effective vibrational reduced masses, μ_{vib} . In the second step, we replace the effective vibrational reduced masses by the effective rotational reduced masses, μ_{rot} , and the rotational and vibrational levels are calculated. In the third step, the pure rotational levels are extracted from the rovibrational level calculation performed in the second step. In the last step the energies of the rovibrational levels are determined by adding the pure rotational levels obtained in the third step to the corresponding pure vibrational levels obtained in the first step.

C. Evaluating the rovibrational transitions

Though the most accurate to date BO PEC of Pachucki¹⁹ is adopted in the present calculation of the rovibrational levels, an issue appeared due to his BO PEC being sparse for $R \geq 20 a_0$ (step size = $10 a_0$). This PEC region near the dissociation limit is important for the high rovibrational levels. To fix the sparsity issue and to obtain a more densely sampled PEC in the $R \geq 20 a_0$ region, we fitted the difference between Pachucki's and our BO PECs, $\Delta E = E_{\text{Pachucki}} - E_{\text{Present}}$, in this region with a polynomial. Then we discretized the polynomial using a grid with a step size of $1 a_0$ and added it to our BO PEC. This sum was then used to replace the 20–60 a_0 region in Pachucki's BO PEC. The PEC obtained this way was then augmented with the ACs calculated in this work and used in the rovibrational calculations.

Table VI compares the pure rotational transitions calculated by Bishop and Cheung¹⁶ with the present values. Due to the limited range of their PEC, the pure rotational levels are only calculated for $\nu \leq 2$. The largest difference between the two calculations is about 0.015 cm^{-1} and both sets of the calculated frequencies show a similar difference with respect to the experimental transitions. This similarity is affirmed by the corresponding root-mean-square errors (RMSEs) differing only by 0.005 cm^{-1} .

Since the accuracy of the rovibrational level calculation depends on the quality of the PEC, let us evaluate the improvement of our PEC over the PEC of Bishop and Cheung. The potential depth is a good indicator of the PEC accuracy. The depth of the Bishop and Cheung's PEC is $16\,456.1442 \text{ cm}^{-1}$ and of ours is $16\,456.6946 \text{ cm}^{-1}$. The difference is only 0.5504 cm^{-1} . This seems to suggest a small improvement; however, a more detail examination reveals larger discrepancies between the two PECs in the mid-region. Table VII shows that the largest and the smallest differences between the two PECs occur at $R = 4.5 a_0$ and $R = \infty$ with the values of -1.549 cm^{-1} and -0.322 cm^{-1} , respectively. Thus, the two PECs, while parallel around the equilibrium bond length, diverge more in the mid-region.

Purder *et al.*⁶ stated that the $\nu = 1 - 0$ rovibrational transitions mainly probe the $1.2\text{--}2.0 a_0$ range of the PEC and the $\nu = 2 - 1$ transitions extend the probing to the $1.1\text{--}2.2 a_0$ range. In order to predict the line positions corresponding to the $\nu = 3 - 2$ transitions in $^4\text{HeH}^+$ and $^4\text{HeD}^+$, Purder *et al.*

TABLE VII. Comparison of the BO PEC and of the adiabatic correction between the present calculations and those of Bishop and Cheung.¹⁶

R (bohrs)	E _{BO} (E _h)	ΔE _{BO} (cm ⁻¹)	E _{ad} (cm ⁻¹)	ΔE _{ad} (cm ⁻¹)
0.9	-2.845 647 01	-0.700	199.699	-0.007
1.2	-2.962 047 46	...	106.576	-0.006
1.46	-2.978 706 59	-0.872	100.286	-0.004
1.8	-2.967 566 12	-1.249	95.953	0.005
2.4	-2.937 111 60	...	93.325	0.014
3.0	-2.918 594 29	-1.300	92.609	0.029
4.5	-2.905 929 17	-1.549	92.081	0.027
6.0	-2.904 314 56	-0.852	92.109	0.000
∞	-2.903 724 38	-0.322	92.455	0.000

readjusted the PEC of Bishop and Cheung to improve the agreement with the experimental data for the $\nu = 1 - 0$ and $\nu = 2 - 1$ transitions. Their and our results are shown in Table IX. Both calculations show similar differences in comparison with the experiment. While it took an empirically adjusted correction added to the Bishop and Cheung PEC to achieve that, our PEC does it without any empirical correction.

Engel *et al.*¹⁷ used the effective reduced masses given by Coxon and Hajigeorgiou² to partially account for the nonadiabatic effects and recalculated the HeH⁺ rovibrational energy levels with the PEC generated by Bishop and Cheung.¹⁶ As shown in Table VIII, their results agree with the experimental data for the low rovibrational transitions, but larger discrepancies are observed for higher rovibrational transitions. Two possible reasons could have caused these larger differences. First, as mentioned by Bishop and Cheung,¹⁶ the relatively small number of points in their PEC could lead to the energy levels above $\nu = 2$ to be less accurate by as much as 0.2 cm⁻¹. The other reason could be the use of a not optimal value of the effective reduced mass. On the other hand, our calculations maintain similar high accuracy for both high and low rovibrational energy levels. For example, the (13,5)-(9,6) and (13,5)-(9,4) rovibrational transitions of ⁴HeD⁺ allow to evaluate the accuracy of the long-range behavior of the PEC. Table IX shows that the differences between the experimental and theoretical energies of these two transitions are -0.023 cm⁻¹ and -0.012 cm⁻¹, respectively. These values indicate that the quality of the PEC is uniformly high for short and long internuclear distances. The results of ³HeH⁺ and ³HeD⁺ are shown in Tables X and XI, respectively.

As mentioned, in the present rovibrational calculations the effective vibrational reduced mass for ⁴HeH⁺ is optimized to match the lowest calculated pure vibrational transition with the value of the transition obtained in the previous direct nonadiabatic calculation. That optimization provided the electron distribution at the two nuclei. In determining the effective reduced masses of the other ⁴HeH⁺ isotopologues the ⁴HeH⁺ electron distribution is used. Even though this is not strictly correct, as the electron distribution should slightly vary between the different isotopologues, this effect can be expected to be small. Due to this approximation the RMSE values for

⁴HeD⁺, ³HeH⁺, and ³HeD⁺ are slightly larger than the value for ⁴HeH⁺.

To assess the quality of the PEC, particularly of its long-range portion, the line width of the transitions involving quasi-bound rovibrational levels are compared with those calculated using the experimental PEC of Coxon and Hajigeorgiou.²

As shown in Table XII, the line widths obtained in the calculation using the *ab initio* PEC agree very well with those calculated with experimental PEC. There are two lines singled out by Coxon and Hajigeorgiou, the (13,5) line of ⁴HeD⁺ and the (6,19) line of ³HeD⁺, which require some analysis. For the (13,5) line of ⁴HeD⁺, the present value falls between the value of Coxon and Hajigeorgiou and the value of Carrington *et al.*⁵ Coxon and Hajigeorgiou state that this line corresponds to a very weakly bound, difficult to calculate state. For the (6,19) line of ³HeD⁺, the present value agrees better with the value of Coxon and Hajigeorgiou than the experimental value. According to Carrington *et al.*,^{2,5} the line is affected by Doppler broadening and possibly power broadening, which can be the reasons for the discrepancy.

It is interesting to compare the experimental BO PEC of Coxon and Hajigeorgiou² and the most accurate to date *ab initio* BO PEC of Pachucki.¹⁹ The difference between the two PECs is shown in Figure 2. The main difference between the two PECs is in the D_e value, which is 16 456.24 cm⁻¹ at R_e = 1.463 279 a₀ for the experimental PEC and 16 457.07 cm⁻¹ at R_e = 1.463 283 a₀ for the *ab initio* PEC. The 0.83 cm⁻¹ difference between the two values is exactly showing in the dissociation limits of the two curves (see the dash line in Figure 2). If one uses the experimental PEC to calculate the rovibrational levels and compares them with the values obtained in the present calculations, the 0.83 cm⁻¹ difference, if it is not uniform throughout the whole PEC range, will be a source of discrepancies between the two calculations. Another source of discrepancies arises due to the relative differences between the two curves (of ~1.11 cm⁻¹) in the R = 1.46–6 a₀ region and (of ~0.18 cm⁻¹)

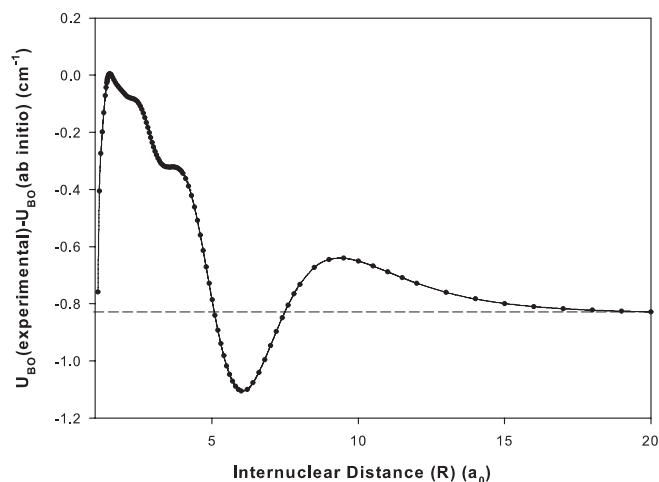


FIG. 2. The difference between the experimental² and the *ab initio*¹⁹ BO PEC for HeH⁺. The dash line represents the 0.83 cm⁻¹ difference of the dissociation limits between two PECs.

TABLE VIII. Difference between the experimental and calculated rovibrational transitions of ${}^4\text{HeH}^+$. All values are in cm^{-1} . $\sigma = \Delta\nu/a$, where a is the measurement uncertainty.

$\nu' - \nu''$	J	P(J)						R(J)					
		Experiment	Purder <i>et al.</i>		Engel <i>et al.</i>		This work		Experiment	Purder <i>et al.</i>		This work	
			$\Delta\nu$	σ	$\Delta\nu$	σ	$\Delta\nu$	σ		$\Delta\nu$	σ	$\Delta\nu$	σ
1 - 0	0								2972.5732 ^a			-0.0611	(-30.5)
	1	2843.9035 ^a			-0.036	(-18.0)	-0.0603	(-30.2)	3028.3750 ^a			-0.0601	(-30.0)
	2	2771.8059 ^a			-0.022	(-11.0)	-0.0556	(-27.8)	3077.9919 ^a			-0.0612	(-30.6)
	3	2695.0500 ^a			-0.002	(-1.0)	-0.0528	(-26.4)	3121.0765 ^a			-0.0612	(-30.6)
	4	2614.0295 ^a			0.020	(10.0)	-0.0509	(-25.4)	3157.2967 ^a			-0.0600	(-30.0)
	5	2529.134 ^b			0.043	(21.5)	-0.048	(-24.0)	3186.337 ^b			-0.062	(-30.8)
	6	2440.742 ^b			0.066	(33.0)	-0.044	(-22.1)	3207.909 ^b			-0.064	(-32.1)
	7								3221.752 ^b			-0.060	(-29.8)
	9	2158.140 ^c	0.037	(12.3)	0.136	(45.3)	-0.032	(-10.8)					
	10	2059.210 ^c	0.058	(19.3)	0.156	(52.0)	-0.029	(-9.7)					
	11	1958.388 ^c	0.080	(26.7)	0.174	(58.0)	-0.027	(-8.8)					
	12	1855.905 ^d			0.195	(65.0)	-0.029	(-9.8)					
	13	1751.971 ^d			0.206	(68.7)	-0.025	(-8.4)					
2 - 1	1	2542.531 ^e			-0.173	(-86.5)	-0.063	(-31.2)	2660.284 ^e			-0.063	(-31.4)
	2	2475.814 ^e			-0.159	(-79.5)	-0.062	(-30.8)	2710.566 ^e			-0.063	(-31.4)
	3								2754.624 ^b			-0.067	(-33.3)
	4								2792.110 ^b			-0.068	(-33.8)
	5	2248.854 ^c	0.106	(35.3)	-0.102	(-34.0)	-0.047	(-15.7)	2822.683 ^b			-0.066	(-32.7)
	6	2165.485 ^c	0.121	(40.3)	-0.072	(-24.0)	-0.046	(-15.6)	2846.009 ^b			-0.067	(-33.5)
	7	2078.841 ^c	0.133	(44.3)	-0.027	(-9.0)	-0.048	(-16.0)	2861.786 ^b			-0.061	(-30.3)
	8	1989.251 ^c	0.148	(49.3)	-0.005	(-1.7)	-0.042	(-14.1)	2869.690 ^b			-0.069	(-34.4)
	9	1896.992 ^d			0.038	(12.7)	-0.047	(-15.8)	2869.478 ^b			-0.041	(-20.5)
	10	1802.349 ^d			0.072	(24.0)	-0.043	(-14.3)					
	11	1705.543 ^d			0.105	(35.0)	-0.036	(-12.1)					
	19	862.529 ^f			0.341	(113.7)	0.026	(8.5)					
	20	745.624 ^f			0.377	(125.7)	0.028	(9.2)					
3 - 2	4								2484.912 ^c	-0.105	(-35.0)	-0.053	(-17.8)
	5	1966.356 ^c	-0.165	(-55.0)	-0.051	(-17.0)	-0.062	(-20.7)	2501.941 ^c	-0.098	(-32.7)	-0.053	(-17.7)
	6								2511.188 ^c	-0.094	(-31.3)	-0.054	(-18.1)
	8								2504.914 ^c	-0.073	(-24.3)	-0.046	(-15.2)
	9								2488.632 ^c	-0.058	(-19.3)	-0.043	(-14.3)
	17	833.640 ^f			0.336	(12.0)	0.001	(0.3)					
	18	719.769 ^f			0.380	(126.7)	0.019	(6.3)					
5 - 4	11	901.963 ^f			0.259	(86.3)	-0.029	(-9.7)					
	12	807.806 ^f			0.309	(103.0)	-0.035	(-11.5)					
6 - 5	8	863.378 ^f			0.252	(84.0)	-0.050	(-16.8)					
	9	782.925 ^f			0.274	(91.3)	-0.038	(-12.5)					
	12								979.904 ⁱ			0.065	(64.5)
7 - 6	4	817.337 ^f			0.342	(114.0)	-0.020	(-6.7)					
	5	760.367 ^g			0.380	(126.7)	-0.039	(-12.9)					
7 - 5	12	938.200 ^h			0.573	(573.0)	0.095	(94.9)					
RMSE ^j			0.114		0.220		0.045			0.087		0.060	

^aBernath and Amano, $a = 0.002 \text{ cm}^{-1}$.⁷^bCrofton *et al.*, $a = 0.002 \text{ cm}^{-1}$.⁹^cPurder *et al.*, $a = 0.003 \text{ cm}^{-1}$.⁶^dTolliver *et al.*, $a = 0.002 \text{ cm}^{-1}$.³^eBlom *et al.*, $a = 0.001 \text{ cm}^{-1}$.⁴⁰^fLiu and Davies, $a = 0.003 \text{ cm}^{-1}$.¹²^gHoyland, $a = 0.003 \text{ cm}^{-1}$.³⁹^hCarrington *et al.*, $a = 0.001 \text{ cm}^{-1}$.⁴ⁱCarrington *et al.*, $a = 0.001 \text{ cm}^{-1}$.⁵^jRoot-mean-square error.

TABLE IX. Difference between experimental and calculated rovibrational transitions of ${}^4\text{HeD}^+$. All values are in cm^{-1} . $\sigma = \Delta\nu/a$, where a is the measurement uncertainty.

$\nu' - \nu''$	J	P(J)					R(J)				
		Experiment	Purder <i>et al.</i>		This work		Experiment	Purder <i>et al.</i>		This work	
			$\Delta\nu$	σ	$\Delta\nu$	σ		$\Delta\nu$	σ	$\Delta\nu$	σ
1-0	0						2348.628 ^a			-0.069	(-34.4)
	1	2269.812 ^a			-0.062	(-31.0)	2384.108 ^a			-0.066	(-33.2)
	2						2416.780 ^a			-0.069	(-34.4)
	3	2181.432 ^a			-0.061	(-30.5)	2446.518 ^a			-0.072	(-36.1)
	4	2134.011 ^b	-0.078	(-26.0)	-0.063	(-21.0)	2473.202 ^a			-0.071	(-35.5)
	5	2084.633 ^b	-0.074	(-24.7)	-0.060	(-20.1)	2496.703 ^a			-0.075	(-37.6)
	6						2516.917 ^a			-0.075	(-37.4)
	7						2533.732 ^a			-0.075	(-37.5)
	8	1926.132 ^b	-0.060	(-20.0)	-0.052	(-17.3)	2547.048 ^a			-0.075	(-37.6)
	9						2556.772 ^a			-0.074	(-36.9)
	10						2562.812 ^a			-0.075	(-37.5)
2-1	1	2088.030 ^b	0.019	(6.3)	-0.069	(-22.8)					
	3						2252.028 ^b	0.037	(12.3)	-0.069	(-22.9)
	4	1959.756 ^b	0.045	(15.0)	-0.056	(-18.8)					
	5						2297.086 ^b	0.055	(18.3)	-0.072	(-24.1)
3-2	4						2078.586 ^b	0.070	(23.3)	-0.061	(-20.4)
	5						2096.816 ^b	0.058	(19.3)	-0.070	(-23.2)
	8						2131.027 ^b	0.032	(10.7)	-0.072	(-24.1)
4-3	9						1920.660 ^b	-0.091	(-30.3)	-0.061	(-20.2)
	12						1899.333 ^b	-0.019	(-6.3)	-0.055	(-18.2)
6-4	22	1088.373 ^c			0.091	(91.5)					
6-5	20						1003.329 ^c			0.066	(65.8)
7-5	20	944.720 ^c			0.100	(99.6)					
13-9	4						1073.475 ^c			-0.013	(-12.9)
	6	911.705 ^c			-0.023	(-23.4)					
RMSE ^d			0.059		0.067			0.056		0.068	

^aCrofton *et al.*, $a = 0.002 \text{ cm}^{-1}$.⁹^bPurder *et al.*, $a = 0.003 \text{ cm}^{-1}$.⁶^cCarrington *et al.*, $a = 0.001 \text{ cm}^{-1}$.⁵^dRoot-mean-square error.TABLE X. Difference between the experimental and the calculated rovibrational transitions of ${}^3\text{HeH}^+$. All values are in cm^{-1} . $\sigma = \Delta\nu/a$, where a is the measurement uncertainty.

$\nu' - \nu''$	J	P(J)				R(J)			
		Experiment	This work		Experiment	This work		Experiment	$\Delta\nu$
			$\Delta\nu$	σ		$\Delta\nu$	σ		
1-0	0				3060.433 ^a	-0.080	(-40.0)		
	1	2923.680 ^a	-0.078	(-38.9)	3119.405 ^a	-0.082	(-40.8)		
	2	2846.775 ^a	-0.072	(-36.2)	3171.549 ^a	-0.083	(-41.5)		
	3	2764.768 ^a	-0.073	(-36.2)	3216.468 ^a	-0.084	(-42.2)		
	4	2678.113 ^a	-0.069	(-34.6)	3253.785 ^a	-0.088	(-43.9)		
	5	2587.243 ^a	-0.068	(-34.2)	3283.156 ^a	-0.086	(-43.1)		
	6	2492.591 ^a	-0.064	(-32.2)	3304.247 ^a	-0.088	(-43.9)		
	7				3316.761 ^a	-0.088	(-43.9)		
6-5	11				981.322 ^b	0.123	(123.1)		
RMSE ^c			0.071			0.090			

^aCrofton *et al.*, $a = 0.002 \text{ cm}^{-1}$.⁹^bCarrington *et al.*,⁵ $a = 0.001 \text{ cm}^{-1}$.^cRoot-mean-square error.

in the $R = 9.5\text{--}20 a_0$ region. The more parallel behavior of the two curves in the $R > 9.5 a_0$ region may explain the better agreement between the results of Coxon and Hajigeorgiou² and the present results for the level widths corresponding to the quasi-bound levels.

TABLE XI. Difference between the experimental and the calculated rovibrational transitions of ${}^3\text{HeD}^+$. All values are in cm^{-1} . $\sigma = \Delta\nu/a$, where a is the measurement uncertainty.

$\nu' - \nu''$	J	P(J)				R(J)			
		Experiment	This work		Experiment	This work		Experiment	$\Delta\nu$
			$\Delta\nu$	σ		$\Delta\nu$	σ		
1-0	1	2378.374 ^a	-0.0785	(-39.2)	2504.487 ^a	-0.0891	(-44.5)		
	2				2540.161 ^a	-0.0937	(-46.8)		
	3	2280.081 ^a	-0.0828	(-41.4)	2572.388 ^a	-0.0938	(-46.9)		
	4				2601.007 ^a	-0.0976	(-48.8)		
6-5	18				1034.144 ^b	0.1452	(145.2)		
7-5	18	995.415 ^b	0.2074	(207.4)					
RMSE ^c			0.137			0.106			

^aCrofton *et al.*, $a = 0.002 \text{ cm}^{-1}$.⁹^bCarrington *et al.*, $a = 0.001 \text{ cm}^{-1}$.⁵^cRoot-mean-square error.

TABLE XII. Level width (in cm^{-1}) of quasi-bound levels of HeH^+ .

	ν	J	Experiment	Coxon and Hajigeorgious	This work		ν	J	Experiment	Coxon and Hajigeorgious	This work	
$^4\text{HeH}^+$	0	26	0.0189 ^a	0.0191	0.0191	$^3\text{HeH}^+$	11	10	0.027 ^b	2.11	2.27	
		27		6.17	6.18		12	7		1.7×10^{-5}	2.1×10^{-5}	
	1	24		0.092 ^a	0.0708		0.0708	13		5	0.0467	0.0352
		25			18.2		18.2	2		22	8.7×10^{-3}	8.6×10^{-5}
	2	22	0.103 ^b	0.214	0.212		0	25	0.029 ^b	4.48	4.44	
		23		26.4	36.5		1	23		0.0303	0.0298	
	3	19		1.45×10^{-6}	1.47×10^{-6}		2	24		13.6	13.5	
		20			0.736		0.738	2		21	0.0900	0.0888
	4	17	4.10 ^b	1.5×10^{-5}	1.52×10^{-5}		2	22	28.2	28.1		
		18		3.13	3.14		3	19	0.343	0.339		
	5	15		8.23×10^{-4}	8.49×10^{-4}		3	20	52.7	52.7		
		16			13.2		13.22	4	17	1.78	1.77	
	6	13	4.10 ^b	0.0978	0.1004		4	17	1.78	1.77		
	7	11		3.61	3.69		5	15	9.57	9.51		
	8	8		1.7×10^{-4}	2.18×10^{-4}		6	12	0.0277	0.0281		
	9	6			0.363		0.397	7	10	2.35	2.40	
$^4\text{HeD}^+$	0	34	1.0×10^{-3b}	9.7×10^{-4}	9.7×10^{-4}	$^3\text{HeH}^+$	0	32	4.5×10^{-4b}	3.70×10^{-4}	3.73×10^{-4}	
		35		0.500	0.500			33		0.322	0.324	
		36		20.7	20.7			34		17.9	17.9	
	1	32			4.3×10^{-3}		4.3×10^{-3}	1		30	1.50×10^{-3}	1.51×10^{-3}
		33	2.07				2.07		31	1.34	1.34	
								32	47.5	47.5		
	2	30	1.0 $\times 10^{-3b}$	0.0136	0.0136		2	28	5.6×10^{-3b}	4.52×10^{-3}	4.56×10^{-3}	
		31		5.35	5.37			29		3.58	3.60	
	3	28		0.0436	0.0437		3	26		0.0150	0.0151	
		29			11.7		11.7			27	8.32	8.38
	4	25	0.018 ^b	2.3×10^{-6}	2.3×10^{-6}		4	24	5.8 ^b	0.0645	0.0650	
		26					0.165	0.165			25	18.3
		27		23.7	23.7		5	22		0.370	0.372	
	5	23		2.0×10^{-5}	2.1×10^{-5}		6	19		3.66×10^{-5}	3.80×10^{-5}	
		24	0.747		0.748			20	2.35	2.36		
	6	21	0.018 ^b	4.2×10^{-4}	4.2×10^{-4}		7	17	5.6×10^{-3b}	3.94×10^{-3}	4.00×10^{-3}	
		22					3.53	3.53			18	11.7
	7	19		0.0156	0.0155		8	15		0.315	0.316	
		20					13.9	13.9		9	13	5.21
	8	17	7.2 $\times 10^{-5}$	0.518	0.515		10	10	0.0315	0.0351		
									11	8	1.12	1.12
	9	14		7.2×10^{-5}	6.08		6.04					
		15						6.08	6.04			
	10	12	0.094	0.099								

^aLiu and Davies.¹¹^bCarrington *et al.*⁵

IV. CONCLUSIONS

Very accurate, dense, and full-range PECs of four HeH^+ isotopologues are generated, and their accuracy is verified by comparing the calculated hot-band rovibrational transitions with the experimental results. Such a comparison tests the quality of the PECs in the whole range of values from the equilibrium to the dissociation limit. It is noticed that the difference between our calculated transition energies and the ex-

perimental values are almost constant. For example, all discrepancies of the R branch transitions of the $\nu = 1 - 0$ band are close to -0.06 cm^{-1} . This value is close to the difference of 0.0588 cm^{-1} between the lowest pure vibrational transition for $^4\text{HeH}^+$ obtained in the nonrelativistic non-BO calculations and its experimental value. As that difference is due to the relativistic and QED effects, it is clear that, in order to further improve the agreement between the calculated and the experimental rovibrational transitions, these effects need

to be included in the calculations. Also, implementation of distance-dependent reduced masses to better account for the nonadiabatic effects would likely benefit the accuracy of the predictions. With that one may expect to achieve a similar accuracy as in the recent calculations of the H_2 rovibrational spectrum,⁴¹ where the leading nonadiabatic, relativistic, and QED corrections were added to the PEC.

ACKNOWLEDGMENTS

We thank Professor M. C. van Hemert for helpful discussions.

- ¹T. R. Hogness and E. G. Lunn, *Phys. Rev.* **26**, 44 (1925).
- ²J. A. Coxon and P. G. Hajigeorgiou, *J. Mol. Spectrosc.* **193**, 306 (1999).
- ³D. E. Tolliver, G. A. Kyrala, and W. H. Wing, *Phys. Rev. Lett.* **43**, 1719 (1979).
- ⁴A. Carrington, J. Buttenshaw, R. A. Kennedy, and T. P. Softley, *Mol. Phys.* **44**, 1233 (1981).
- ⁵A. Carrington, R. A. Kennedy, T. P. Softley, and P. G. Fournier, *Chem. Phys.* **81**, 251 (1983).
- ⁶J. Purder, S. Civis, C. E. Blom, and M. C. van Hemert, *J. Mol. Spectrosc.* **153**, 701 (1992).
- ⁷P. Bernath and T. Amano, *Phys. Rev. Lett.* **48**, 20 (1982).
- ⁸D. J. Liu, W. C. Ho, and T. Oka, *J. Chem. Phys.* **87**, 2442 (1987).
- ⁹M. W. Crofton, R. S. Altman, N. N. Haese, and T. Oka, *J. Chem. Phys.* **91**, 5882 (1989).
- ¹⁰F. Matsushima, T. Oka, and K. Takagi, *Phys. Rev. Lett.* **78**, 1664 (1997).
- ¹¹Z. Liu and P. B. Davies, *Phys. Rev. Lett.* **79**, 2779 (1997).
- ¹²Z. Liu and P. B. Davies, *J. Chem. Phys.* **107**, 337 (1997).
- ¹³L. Wolniewicz, *J. Chem. Phys.* **43**, 1087 (1965).
- ¹⁴W. Kolos, *Int. J. Quantum Chem.* **10**, 217 (1976).
- ¹⁵W. Kolos and J. M. Peek, *Chem. Phys.* **12**, 381 (1976).
- ¹⁶D. M. Bishop and L. M. Cheung, *J. Mol. Spectrosc.* **75**, 462 (1979).
- ¹⁷E. A. Engel, N. Doss, G. J. Harris, and J. Tennyson, *Mon. Not. R. Astron. Soc.* **357**, 471 (2005).
- ¹⁸W. Cencek, J. Komasa, and J. Rychlewski, *Chem. Phys. Lett.* **246**, 417 (1995).
- ¹⁹K. Pachucki, *Phys. Rev. A* **85**, 042511 (2012).
- ²⁰M. Pavanello, S. Bubin, M. Molski, and L. Adamowicz, *J. Chem. Phys.* **123**, 104306 (2005).
- ²¹S. Bubin, M. Stanke, D. Kędziera, and L. Adamowicz, *Phys. Rev. A* **76**, 022512 (2007).
- ²²M. Stanke, D. Kędziera, M. Molski, S. Bubin, M. Barysz, and L. Adamowicz, *Phys. Rev. Lett.* **96**, 233002 (2006).
- ²³M. Stanke, D. Kędziera, S. Bubin, and L. Adamowicz, *Phys. Rev. A* **77**, 022506 (2008).
- ²⁴W. C. Tung, M. Pavanello, and L. Adamowicz, *J. Chem. Phys.* **133**, 124106 (2010).
- ²⁵W. C. Tung, M. Pavanello, and L. Adamowicz, *J. Chem. Phys.* **134**, 064117 (2011).
- ²⁶W. C. Tung, M. Pavanello, and L. Adamowicz, *J. Chem. Phys.* **136**, 104309 (2012).
- ²⁷M. Pavanello, W. C. Tung, and L. Adamowicz, *J. Chem. Phys.* **131**, 184106 (2009).
- ²⁸S. Bubin, M. Cafiero, and L. Adamowicz, *Adv. Chem. Phys.* **131**, 377 (2005).
- ²⁹W. Cencek and W. Kutzelnigg, *Chem. Phys. Lett.* **266**, 383 (1997).
- ³⁰N. C. Handy, Y. Yamaguchi, and H. F. Schaefer, *J. Chem. Phys.* **84**, 4481 (1986).
- ³¹Codata 2006 recommended values of the fundamental physical constants.
- ³²See supplementary material at <http://dx.doi.org/10.1063/1.4759077> for the BO PEC energies and adiabatic corrections, as well as all the values of all the rotational-vibrational energy levels of HeH^+ .
- ³³R. Jaquet and W. Kutzelnigg, *Chem. Phys.* **346**, 69 (2008).
- ³⁴P. R. Bunker and R. E. Moss, *Mol. Phys.* **33**, 417 (1977).
- ³⁵P. R. Bunker, C. J. McLarnon, and R. E. Moss, *Mol. Phys.* **33**, 425 (1977).
- ³⁶R. J. L. Roy, *A Computer Program for Solving the Radial Schrödinger Equation for Bound and Quasibound Levels* (University of Waterloo, Waterloo, Ontario, Canada, 2007).
- ³⁷M. Stanke, D. Kędziera, S. Bubin, and L. Adamowicz, *J. Chem. Phys.* **126**, 194312 (2007).
- ³⁸G. W. F. Drake, *Handbook of Atomic, Molecular, and Optical Physics*, edited by G. W. F. Drake (Springer, 2006).
- ³⁹J. R. Hoyland, *J. Chem. Phys.* **47**, 49 (1967).
- ⁴⁰C. E. Blom, K. Möller, and R. R. Filgueira, *Chem. Phys. Lett.* **140**, 489 (1987).
- ⁴¹J. Komasa, K. Piszczatowski, G. Łach, M. Przybytek, B. Jeziorski, and K. Pachucki, *J. Chem. Theory Comput.* **7**, 3105 (2011).